Biochimica et Biophysica Acta, 1024 (1990) 89–94
Elsevier

BBAMEM 74830

Spin label ESR and ^{31}P-NMR studies of the cubic and inverted hexagonal phases of dimyristoylphosphatidylcholine/myristic acid (1 : 2, mol/mol) mixtures

Y.V.S. Rama Krishna and Derek Marsh

Max-Planck-Institut für biophysikalische Chemie, Abteilung Spektroskopie, Göttingen (F.R.G.)

(Received 16 November 1989)

Key words: Fatty acid; Spin label; Hexagonal H_{II} phase; Cubic phase; ESR; NMR, ^{31}P-

The thermotropic phase behaviour and chain dynamics of the dimyristoylphosphatidylcholine/myristic acid (1:2, mol/mol) mixture at pH 4.0 have been studied with ^{31}P-NMR and spin-label ESR. Broadline proton-dipolar decoupled ^{31}P-NMR spectra show that the system undergoes a transition from a lamellar phase to a non-lamellar phase at 47°C. The ^{31}P-NMR spectrum collapses, from a lamellar powder pattern with apparent chemical shift anisotropy $\Delta\sigma = -38$ ppm below 47°C, to an isotropic spectrum with superimposed hexagonal powder pattern of $\Delta\sigma = +13$ ppm above 47°C. With increasing temperature, the hexagonal component grows at the expense of the isotropic component, finally transforming to a single hexagonal phase at approximately 70°C. The ESR spectra from both fatty acid and phosphatidylcholine probes spin-labelled in the hydrocarbon chain have been used to study the ordering and mobility of the lipid chains through the lamellar-non lamellar transition. An abrupt increase in the chain mobility observed at approx. 47°C demonstrates that the lamellar-non lamellar phase transition coincides with chain melting. The apparent order parameter and polarity profiles, deduced from the ESR spectra of 11 different chain-labelled positional isomers, demonstrate flexibility and polarity gradients characteristic of a lyotropic liquid crystalline phase. The temperature dependence of the order parameters does not show any changes in the fluid phase, indicating that the conversion from the isotropic (cubic) phase to the inverted hexagonal phase is not accompanied by large changes in chain order. A comparison of the apparent order parameters and polarity profiles of the phosphatidylcholine and fatty acid spin labels indicates that the fatty acid spin labels are intercalated approximately one CH_2 unit more deeply in the hydrocarbon region than are the positionally isomeric phosphatidylcholine spin labels.

Introduction

Many phospholipid systems form non-bilayer structures such as the inverted-hexagonal and inverted-cubic types. These phases and the transitions from bilayer to non-bilayer structures are of major interest due to the relevance of these structures in membrane fusion and other membrane mediated processes [1–4]. Among others, the lamellar-hexagonal transitions in various systems have previously been studied by X-ray diffraction, NMR, differential scanning calorimetry and by spin label ESR spectroscopy [5–13]. These studies have established the nature and conditions for the occurrence of the hexagonal phases. In addition, the spin-label studies have revealed increased motional disorder from the headgroup towards the terminal end of the acyl chains in the hexagonal phases (Ref. 6; and Seddon, J.M. and Marsh, D., unpublished data).

The 2 : 1 (mol/mol) stoichiometric mixtures of fatty acids with phosphatidylcholines of the same chain length are known to undergo sharp thermotropic transitions from a lamellar gel to non-lamellar fluid phases. In the case of the palmitic acid system, the chain melting transition takes place directly from a lamellar to an inverted hexagonal phase [5,14]. The investigation of the chain order of the different components in such non-lamellar phases is of considerable relevance to the mode of chain packing in inverted lipid phases and membrane fusion intermediates.

Abbreviations: DMPC, 1,2-dimyristoyl-*sn*-glycero-3-phosphocholine; MA, myristic acid; *n*-SASL, *n*-(4,4-dimethyloxazolidine-*N*-oxyl)stearic acid; *n*-PCSL, 1-acyl-2-[*n*-(4,4-dimethyloxazolidine-*N*-oxyl)stearoyl-*sn*-glycero-3-phosphocholine; CSA, chemical shift anisotropy.

Correspondence: D. Marsh, Max-Planck-Institut für biophysikalische Chemie, Abteilung Spektroskopie, D-3400 Göttingen, F.R.G.

In the present paper, we have investigated the lamellar-non lamellar thermotropic phase transitions in a DMPC/MA (1 : 2, mol/mol) mixture, using ^{31}P-NMR to study the phase properties, and spin label ESR to follow the chain dynamics. The ^{31}P-NMR results indicate a more complex non-lamellar phase behaviour than in the palmitic acid system. The ESR experiments were performed using lipid spin labels with the nitroxide radical at different positions in the acyl chain to study the ordering and relative location of the lipid chains in the two different, coexisting non-lamellar phases.

Materials and Methods

Dimyristoylphosphatidylcholine and myristic acid were obtained from Fluka, Buchs, Switzerland. Stearic acid spin label positional isomers, *n*-SASL, were synthesized as described in Ref. 15. The corresponding phosphatidylcholine spin label isomers, *n*-PCSL, were prepared as described in Ref. 16.

For ^{31}P-NMR measurements, typically 25 mg of the lipid was co-dissolved with twice the molar amount of myristic acid (approx. 16.8 mg) in $CHCl_3/CH_3OH$ (2 : 1, v/v). The solvent was then evaporated off under nitrogen and the sample left under vacuum over night to remove the last traces of the solvent. The mixture was then hydrated with excess of 50 mM sodium acetate buffer and the pH adjusted to 4.0. The sample was then pelleted in a 10-mm NMR tube, using a bench centrifuge, and the excess supernatant buffer removed.

Proton-dipolar decoupled 109 MHz ^{31}P-NMR spectra were recorded on a Bruker WH-270 FT-NMR spectrometer, with a 200 W transmitter, operating in the Fourier-transform mode. Free induction decays were collected with phase cycling, using an rf pulse width of 10 μs and a gated decoupling power of 5–10 W. The duty cycle of the gated decoupling was 0.2% (5 s recycle delay). A sufficient number of scans to ensure adequate S/N ratio was accumulated, typically 300–1000. The sample temperature was measured in the probehead using the standard thermocouple, with an absolute precision estimated to be better than 2 K. A waiting time of 15–20 min was used between points to ensure adequate temperature equilibration.

The ESR experiments were performed on a Varian E-12 9 GHz spectrometer equipped with a nitrogen flow temperature regulation. For these measurements 0.5 mol% spin label was added to 4 ml of a 1 mg/ml solution of DMPC + MA (1 : 2, mol/mol) in $CHCl_3/CH_3OH$ (2 : 1, v/v). The solvent removal and preparation of the sample were as described for the NMR experiments. Typically, samples of height $\approx$ 15 mm were pelleted in 1 mm diameter capillary tubes which were then sealed and housed in 3-mm quartz tubes containing silicone oil for maintaining uniformity of temperature. The sample temperature was measured with a NiCr-Ni thermocouple within the silicone oil at the top of the microwave cavity. The expressions used for the apparent order parameter, S^{app}, and the apparent isotropic coupling constant, a_0^{app}, are given by [17]:

$$S^{app} = (A_{\parallel} - A_{\perp})/[A_{zz} - \tfrac{1}{2}(A_{xx} + A_{yy})](a_0'/a_0) \quad (1)$$

$$a_0^{app} = (1/3)(A_{\parallel} + 2A_{\perp}) \quad (2)$$

where $A_{\parallel}$ is A_{max}, half of the outer hyperfine splitting, and $A_{\perp}$ is obtained from A_{min}, which is half of the inner hyperfine splitting, according to [18]:

$$A_{\perp}(G) = A_{min}(G) + 1.4[1 - (A_{\parallel} - A_{min})/(A_{zz} - (1/2)(A_{xx} + A_{yy}))] \quad (3)$$

A_{xx}, A_{yy} and A_{zz} are the principal values of the hyperfine tensor in the nitroxide frame of axes, obtained from measurements in a single crystal environment [19], and

$$a_0' = (1/3)(A_{xx} + A_{yy} + A_{zz}) \quad (4)$$

Detailed simulations of the ESR spectra of chain-labelled lipids have demonstrated the presence of long axis motions in the slow motional regime in fluid phase bilayers [20,21]. Therefore, the order parameters calculated from Eqn. 2, using motional narrowing theory, are only apparent values, which will approximate the ordering associated with fast chain motions, viz. *trans-gauche* isomerism. These parameters can be used empirically to compare the dynamic properties of the fatty acid and phosphatidylcholine components in the fluid phase.

Results and Discussion

The proton-dipolar decoupled ^{31}P-NMR spectra of a DMPC/MA (1 : 2, mol/mol) dispersion at pH 4.0, recorded at different temperatures, are shown in Fig. 1. The low-temperature spectra are broad and axially symmetric with a large effective chemical shift anisotropy (CSA) of $\Delta\sigma \approx -55$ ppm at 10 °C, characteristic of a gel phase bilayer arrangement. As the temperature is increased the CSA decreases gradually until 47 °C, at which temperature the chemical shift anisotropy decreases drastically and a strong isotropic resonance dominates the spectrum. This isotropic resonance is superimposed upon a spectrum with positive CSA: $\Delta\sigma \approx +13$ ppm. As the temperature is increased further, the intensity of the isotropic component decreases with a concomitant increase in the intensity of the other component, which is characteristic of phospholipids in the inverted-hexagonal (H_{II}) phase [1,5]. By approx. 76 °C, the system transforms completely into a pure hexagonal phase with $\Delta\sigma \approx +15$ ppm. The large decrease in the anisotropy of the spectrum in the hexago-

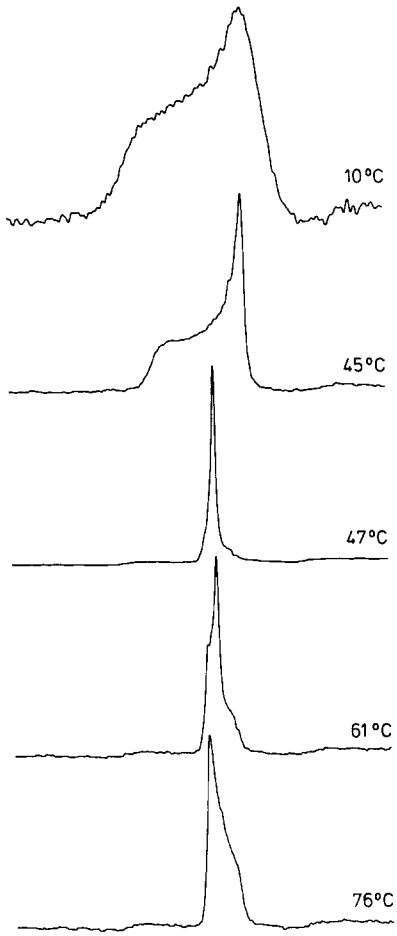

Fig. 1. Proton-dipolar decoupled 109 MHz ^{31}P-NMR spectra of a DMPC/MA (1:2, mol/mol) mixture at pH 4.0. Spectra were recorded at the temperatures indicated. Total plot width = 160 ppm.

nal phase is partly due to motional averaging by rapid lateral diffusion around the cylinder axis. In the absence of this additional motion, the equivalent CSA would be: $\Delta\sigma \approx -30$ ppm. ^{31}P-NMR is not diagnostic in determining the identity of the isotropic phase, although the spectra are consistent with a liquid crystalline phase of cubic symmetry. The reversible conversion to the H_{II} phase at higher temperature further supports the assignment to a cubic phase. Very recent X-ray diffraction measurements have identified this phase as one with the cubic space group *Pn3m* or possibly *Im3m* [22,27].

Fig. 2 shows the temperature dependence of the effective chemical shift anisotropy, measured as the difference in the chemical shifts between the points of maximum slope. At low temperatures, in the lamellar phase, the value of the CSA starts at $\Delta\sigma \approx -56$ ppm. It decreases over a broad transition range to $\Delta\sigma \approx -38$ ppm at 40 °C. A similar, large temperature dependence of the CSA was observed previously in the gel phase of the system with palmitoyl chains [5], and most probably corresponds to additional motional freedom allowed by spacing of the phospholipid headgroups by the intercalated fatty acid. At 47 °C, a sharp transition takes place to a non-lamellar phase. This phase is initially isotropic (cubic), but with increasing temperature it gradually converts to an inverted hexagonal phase. In view of the relatively long time span of the experiments (cf. Materials and Methods), it is most likely that the coexisting phases are close to equilibrium. In addition, the changes were reversible on decreasing temperature. The approximate region of phase coexistence is indicated in Fig. 2. Most probably, the H_{II} phase is not present at the transition itself, although the coexistence of three phases cannot be excluded by the phase rule [23].

Two series of spin labels, *n*-SASL and *n*-PCSL ($n = 4$ to 14), with the nitroxide radical at various positions down the acyl chain, have been used for the ESR studies of the transition and of the fluid non-lamellar phases. The ESR spectra of the phosphatidylcholine spin label, 5-PCSL, in the DMPC/MA (1:2, mol/mol) mixture are shown in Fig. 3, for various temperatures. At low temperature, the spectra are entirely in the slow motional regime, and possess close to the rigid limit hyperfine anisotropy. The outer hyperfine splitting, $2A_{max}$, decreases only slowly with increasing temperature until 45 °C, and then decreases abruptly, corresponding to the chain melting phase transition. Above the transition, the spectra possess the characteristic, motionally averaged, axial hyperfine anisotropy of a fluid liquid crystalline phase (cf. ref. 17). Interestingly, the spectrum recorded at 45 °C contains a superposition of the two components characteristic of the fluid and gel phases (Fig. 3).

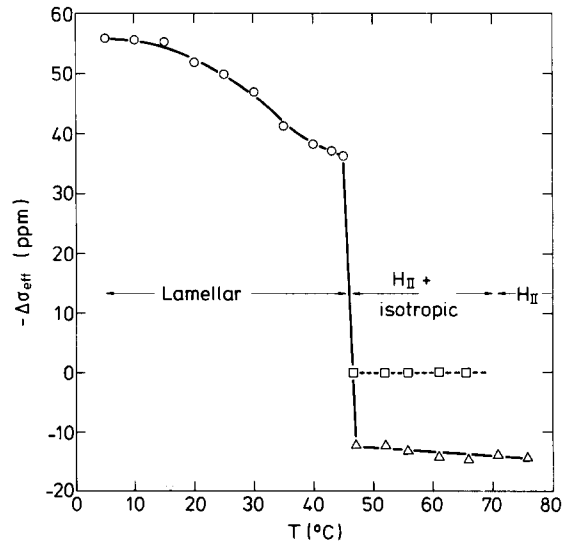

Fig. 2. Temperature dependence of the effective ^{31}P chemical shift anisotropy of a DMPC/MA (1:2, mol/mol) dispersion at pH 4.0. Lamellar phase (○); isotropic phase (□); inverted hexagonal phase (△). Regions of phase coexistence are indicated.

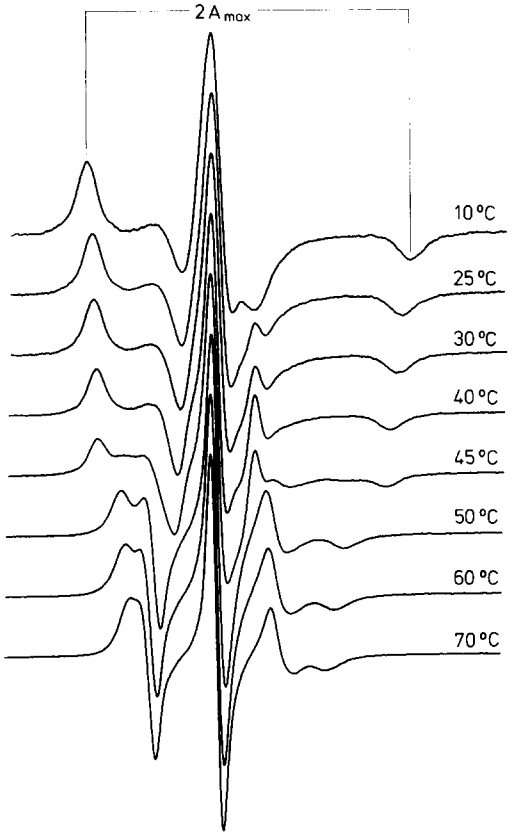

Fig. 3. ESR spectra of the 5-PCSL phosphatidylcholine spin label in a DMPC/MA (1:2, mol/mol) mixture at pH 4.0. Spectra were recorded at the temperatures indicated. Total scan width = 100 gauss.

The temperature dependence of the outer hyperfine splitting constant for different positional isomers of both the phosphatidylcholine and fatty acid spin labels is given in Fig. 4. The *n*-PCSL labels all show that a sharp chain melting transition occurs at approximately 47 °C. The lamellar-non lamellar phase transition detected in the ^{31}P-NMR measurements therefore coincides with the gel-to-fluid chain melting transition. The *n*-SASL labels correspondingly register the same transition, although the 9-SASL label registers a slightly lower transition temperature. The continuity of the temperature dependence of S^{app} above the phase transition suggests that the interconverting cubic and H_{II} phases have a similar degree of chain order. This is consistent with models in which both non-lamellar phases are built from similar structural elements, namely inverted lipid-water cylinders [23,24]. More precisely, the cubic phases are thought to be bicontinuous and related topologically to the lipid bilayer [10,24,25], but possess a curvature stability that is similar to that of H_{II} phases [10,26]. It could be that the degree of chain order is directly related to the latter.

Fig. 5 gives a comparison between the ESR spectra of the fatty acid and phosphatidylcholine spin labels for given positional isomers, *n*-PCSL and *n*-SASL, respectively. The spectra from both sets of labels reflect a clear chain flexibility gradient in the fluid phase, with the spectral anisotropy steadily decreasing with increasing *n*. In each case, however, the ESR spectrum from the phosphatidylcholine spin label has consistently a greater anisotropy than that from the corresponding stearic acid spin label with the same value of *n*.

The positional dependence of the apparent isotropic splitting factor, a_0^{app}, and of the apparent order parameter, S^{app}, at 60 °C for both the *n*-SASL and *n*-PCSL labels is given in Fig. 6. The order parameter profile for both the fatty acid and phosphatidylcholine spin labels reveals a steadily increasing segmental motion down the acyl chain [17]. However, the apparent order parameters for the fatty acid spin labels are somewhat smaller than for the corresponding positional isomers of the phosphatidylcholine spin label. Since the overall shape of the profiles is very similar, this suggests that the protonated fatty acid is located deeper in the hydrophobic region of the phase than is the phosphatidylcholine *sn*-2 chain. Quantitative alignment of the two profiles (Fig. 6C,D) indicates that the fatty acid spin labels are shifted by approximately one CH_2 unit relative to the phosphatidylcholine acyl chain, in the direction of the terminal methyl group.

The polarity profile derived from the apparent isotropic hyperfine coupling constant gives another means

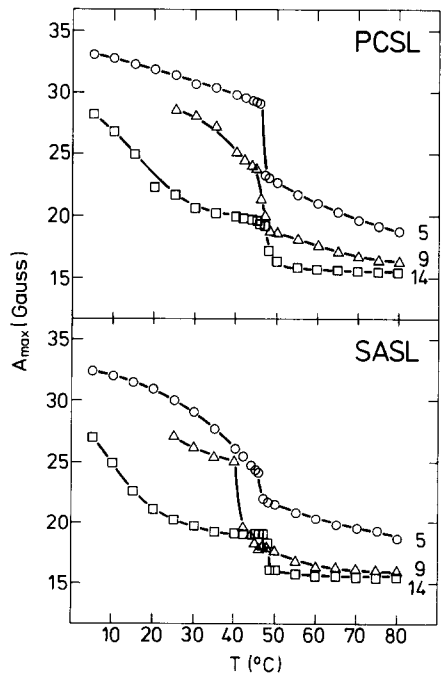

Fig. 4. Temperature dependence of the outer hyperfine splitting, A_{max}, in the ESR spectra of the phosphatidylcholine (*n*-PCSL) and stearic acid (*n*-SASL) spin labels in a DMPC/MA (1:2, mol/mol) mixture at pH 4.0 (Upper panel) Phosphatidylcholine spin labels 5-, 9- and 14-PCSL. (Lower panel) Stearic acid spin labels 5-, 9- and 14-SASL.

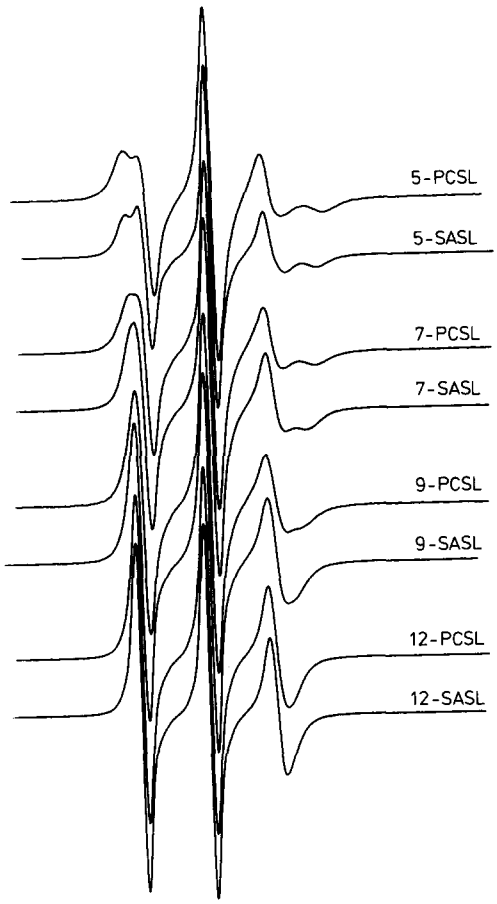

Fig. 5. ESR spectra of the phosphatidylcholine (*n*-PCSL) and stearic acid (*n*-SASL) spin labels in DMPC/MA (1 : 2, mol/mol) mixture at pH 4.0, recorded at 60 °C. The upper spectrum of each pair is *n*-PCSL and the lower spectrum of each pair is *n*-SASL. Total scan width = 100 gauss.

of locating the position of the label. The value of a_0^{app} decreases steadily with the distance of the nitroxide radical from the polar headgroup region, with a relative flattening off at the positions C12–C14 (Fig. 6A,B). This profile of the environmental polarity is similar for both phosphatidylcholine and stearic acid spin labels and corresponds to the extent of water penetration into the apolar region of the phase. The a_0^{app} profile for the *n*-SASL labels is shifted by approximately one CH_2 group relative to that of the *n*-PCSL labels, in the same direction as for the order parameter profile *. The finding that the fatty acid is located deeper into the

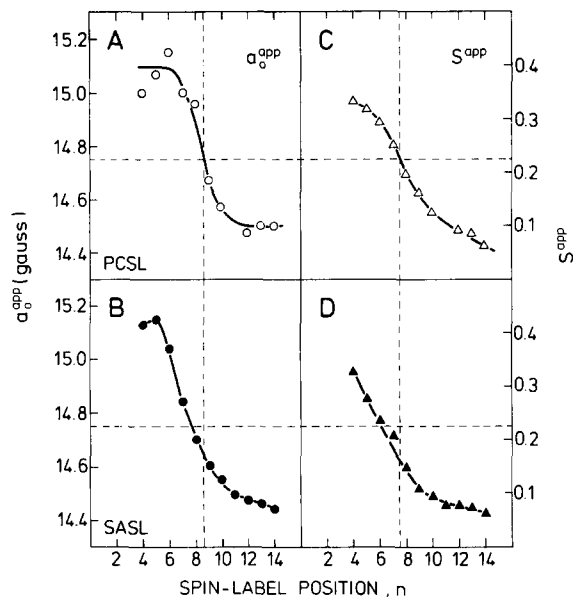

Fig. 6. Positional dependence of (A, B) the apparent isotropic splitting constant, a_0^{app}, and (C, D) the apparent order parameter, S^{app}, of the *n*-PCSL (A, C) and *n*-SASL (B, D) spin labels in DMPC/MA (1 : 2, mol/mol) mixture at pH 4.0 and a temperature of 60 °C. The dashed lines facilitate comparison of label positions corresponding to the same value of a_0^{app} or S^{app}, indicating the relative displacement between *n*-PCSL and *n*-SASL.

hydrophobic region than the phosphatidylcholine *sn*-2 chain is of interest with respect to the structure of the inverted phases. Varying lipid lengths are present in these phases, and it may be that differing degrees of chain intercalation between the two components best satisfy these packing restraints, hence favouring formation of the inverted phase.

In summary, the structure of the fluid phase of the phosphatidylcholine/fatty acid (1 : 2, mol/mol) mixture with myristoyl chains differs from that with palmitoyl chains, consisting of a coexisting cubic and inverted hexagonal phase. However, both non-lamellar phases display rather similar chain ordering, consistent with both being composed essentially of water-containing inverted lipid cylinders (H_{II} and cubic, respectively).

References

1 De Kruijff, B., Cullis, P.R., Verkleij, A.J., Hope, M.J., Van Echteld, C.J.A. and Taraschi, T.F. (1984) in Enzymes of Biological Membranes (Martonosi, A., ed.), Vol. 5, pp. 131–204, Plenum Press, New York.
2 Marsh, D. (1986) in Supramolecular Structure and Function (Pifat-Mrzjlak, G., ed.), pp. 38–47, Springer-Verlag, Berlin.
3 Siegel, D.P. (1986) Biophys. J. 49, 1155–1170.
4 Siegel, D.P. (1986) Biophys. J. 49, 1171–1183.
5 Marsh, D. and Seddon, J. (1982) Biochim. Biophys. Acta 690, 117–123.
6 Hardman, P.D. (1982) Eur. J. Biochem. 124, 95–101.
7 Seddon, J.M., Kaye, R.D. and Marsh, D. (1983) Biochim. Biophys. Acta 734, 347–352.
8 Seddon, J.M., Cevc, G. and Marsh, D. (1983) Biochemistry 22, 1280–1289.

* This relative location of the fatty acid chains probably results from unfavourable interactions of the protonated carboxyl group at the polar interface. This effect, together with the low fatty acid headgroup to chain volume ratio, provides the driving force for creation of the inverted fluid phase. In the gel phase, there are indications from the relative values of A_{max} (see Fig. 4) that the fatty acid chains may be located more deeply into the hydrophobic region than is the phosphatidylcholine *sn*-2 chain also in the lamellar structure. This latter point is, however, less certain.

9 Seddon, J.M., Cevc, G., Kaye, R.D. and Marsh, D. (1984) Biochemistry 23, 2634–2644.
10 Gruner, S.M., Tate, M.W., Kirk, G.L., So, P.T.C., Turner, D.C., Keane, D.T., Tilcock, C.P.S. and Cullis, P.R. (1988) Biochemistry 27, 2853–2866.
11 Killian, J.A. and De Kruijff, B. (1985) Biochemistry 24, 7881–7890.
12 Ellens, H., Bentz, J. and Szoba, F.C. (1986) Biochemistry 25, 4141–4147.
13 Tilcock, C.P.S., Cullis, P.R. and Gruner, S.M. (1986) Chem. Phys. Lipids 40, 47–56.
14 Kohn, A.B. and Schullery, S.E. (1985) Chem. Phys. Lipids 37, 143–153.
15 Hubbell, W.L. and McConnell, H.M. (1971) J. Am. Chem. Soc. 93, 314–326.
16 Marsh, D. and Watts, A. (1982) in Protein-Lipid Interactions (Jost, P.C. and Griffith, O.H., eds.), Vol. 2, pp. 53–156, Wiley-Interscience, New York.
17 Marsh, D. (1981) in Membrane Spectroscopy (Grell, E., ed.), pp. 51–142, Springer-Verlag, Berlin.
18 Griffith, O.H. and Jost, P.C. (1976) in Spin Labelling-Theory and Applications (Berliner, L.J., ed.). pp. 453–523, Academic Press, New York.
19 Jost, P.C., Libertini, L.J., Herbert, V.C. and Griffith, O.H. (1971) J. Mol. Biol. 59, 77–98.
20 Lange, A., Marsh, D., Wassmer, K.-H., Meier, P. and Kothe, G. (1985) Biochemistry 24, 4383–4392.
21 Moser, M., Marsh, D., Meier, P., Wassmer, K.-H. and Kothe, G. (1989) Biophys. J. 55, 111–123.
22 Ryba, N.J.P., Heimburg, T. and Marsh, D. (1989) Biophys. J. 55, 248a.
23 Cevc, G. and Marsh, D. (1987) Phospholipid Bilayers, Physical Principles and Models, 442 pp., Wiley-Interscience, New York.
24 Mariani, P., Luzzati, V. and Delacroix, H. (1988) J. Mol. Biol. 204, 165–189.
25 Longley, W. and McIntosh, T.J. (1983) Nature 303, 612–614.
26 Anderson, D.M., Gruner, S.M. and Leibler, S. (1988) Proc. Natl. Acad. Sci. USA 85, 5364–5368.
27 Heimburg, T., Ryba, N.J.P., Würz, U. and Marsh, D. (1990) Biochim. Biophys. Acta 1025, in press.